JPET Fast Forward. Published on January 30, 2017 as DOI: 10.1124/jpet.116.238469
This article has not been copyedited and formatted. The final version may differ from this version.



**Title page**

# Control of Neurotransmission by NaV1.7 in Human, Guinea pig, and Mouse airway Parasympathetic Nerves

Kocmalova, M., Kollarik,M., Canning, B.J., Ru, F., Herbstromer, R.A., Meeker, S., Fonquerna, S., Aparici, M., Miralpeix, M., Chi, X., Li B., Wilenkin B., McDermott, J., Nisenbaum, E., Krajewski, J.L., and Undem, B.J.

Johns Hopkins University School of Medicine, Division of Allergy and Clnical Immunology, Baltimore Maryland, USA (MKoc, MK, BJC, FR, RAH, SM, BJU)

Biomedical Center Martin, Pharmacology & Pathophysiology, Jessenius Faculty of Medicine, Comenius University, Martin, Slovakia (MKoc, MK)

Almirall S.A., R&D Research Center, Barcelona, Spain (SF, MA, MM)

Lilly Research Laboratories, Indianapolis, IN USA (XC, BL, BW, JM, EN, JLK)

Running Title

NaV1.7 controls bronchial parasympathetic neurotransmission.

*Corresponding Author*

Bradley Undem

JHU Asthma Center

5501 Hopkins Bayview Circle

Baltimore, MD 21224

bundem@jhmi.edu

Statistics

Pages = 22

Tables = 3

Figures = 3

References = 20

Abstract = 198 words

Introduction = 308 words

Discussion = 818 words

Nonstandard Abbreviations
NaV – voltage gated sodium channel
TTX-tetrodotoxin
COPD-chronic obstructive pulmonary disorder

Abstract:

Little is known about the voltage-gated sodium channels (NaVs) that control neurotransmission in the parasympathetic nervous system. We evaluated the expression of the α subunits of each of the nine NaVs in human, guinea pig, and mouse airway parasympathetic ganglia. We combined this information with a pharmacological analysis of selective NaV blockers on parasympathetic contractions of isolated airway smooth muscle. As would be expected from previous studies, tetrodotoxin potently blocked the parasympathetic responses in the airways of each species. Gene expression analysis showed that that NaV 1.7 was virtually the only tetrodotoxin-sensitive NaV1 gene expressed in guinea pig and human airway parasympathetic ganglia, where mouse ganglia expressed NaV 1.1, 1.3, and 1.7. Using selective pharmacological blockers supported the gene expression results showing that blocking NaV 1.7 alone can abolish the responses in guinea pig and human bronchi, but not in mouse airways. To block the responses in mouse airways requires that NaV 1.7 along with NaV1.1 and/or NaV 1.3 is blocked. These results may suggest novel indications for NaV1.7 blocking drugs where there is an overactive parasympathetic drive such as in asthma. The data also raise the potential concern of anti-parasympathetic side effects for systemic NaV 1.7 blockers.

## Introduction

The pore forming $\alpha$ subunits of voltage-gated sodium channels comprise nine distinct subtypes referred to as NaV1.1 – 1.9. With respect to the peripheral nervous system they have been extensively investigated in sensory nerves, but much less so in autonomic nerves; and virtually not all in the parasympathetic nervous system. The parasympathetic nervous system controls the function of visceral organs. In the respiratory tract, parasympathetic nerves regulate secretions and provide the dominant control over airway smooth muscle tone and airway caliber. Dysregulation of this system can contribute to airway inflammatory diseases like asthma and COPD (Undem and Potenzieri, 2012).

Other than the fact that they are generally blocked by tetrodotoxin (TTX), little is known about the neuronal voltage-gated sodium channels (NaV1s) involved in parasympathetic neurotransmission in visceral organs. We have addressed this question here by focusing on the postganglionic parasympathetic nerves controlling airway caliber. TTX potently blocks NaV1.1, NaV1.2, NaV1.3, NaV1.4, NaV1.6, and NaV1.7. Among these all but NaV1.4 are expressed by peripheral neurons. Which of these channels are responsible for the TTX-sensitive neuronal cholinergic airway contractions is unknown.

We evaluated the functionality of these channels in airway cholinergic responses using selective NaV1 blocking drugs along with an evaluation of NaV1 gene expression in isolated bronchial associated parasympathetic ganglia in guinea pigs, mice, and humans. The data support the conclusion that airway parasympathetic cholinergic neurotransmission is entirely dependent on NaV1.7 in humans and guinea pigs, but not mice. This information is significant because NaV 1.7 is associated with channelopathies that can lead to a gain or loss of function (Waxman, 2013). In addition, selective NaV 1.7 blockers are presently being developed aimed at

controlling pain (Priest and Kaczorowski, 2007). That NaV 1.7 controls parasympathetic nerve function may provide additional therapeutic targets for NaV1.7 blockers, as well as help explain potential unwanted anti-parasympathetic side-effects when these drugs are used systemically.

## Methods

The experimental protocols for guinea pig and mouse experiments were approved by the Johns Hopkins University Animals Care and Use Committee

Tissue bath Studies

*Guinea Pig Trachea*

Male Hartley guinea pigs (100–200 g) were obtained from Hilltop Laboratory Animals, Inc., Scottsdale, PA, USA). The animals were killed by CO2 asphyxiation. The trachea was removed and placed in Kreb's bicarbonate buffer composed of (in mM): 118 sodium chloride, 5.4 KCl, 1.0 $NaH_2PO_4$, 1.2 $MgSO_4$, 1.9 $CaCl_2$, 25 $NaHCO_3$, 11.1 glucose equilibrated with 95% $O_2$–5% $CO_2$ (pH 7.4). After trimming the trachea free of extraneous tissue, it was cut into segments comprising ~4 cartilagenous rings. The preparations were connected to force-displacement transducers for measurements of isometric tension responses. They were equilibrated under 1 gram of resting tension for 90 min in water-jacketed tissue baths containing Kreb's buffer maintained at 37oC, with the buffer replaced at 15 min intervals. Platinum wires, connected to a Grass S48 stimulator were positioned on either side of the tissue segments. Propranolol (1 μM) and indomethacin (3 μM) were added to the buffer at the beginning of the experiment to reduced the influence of beta adrenergic responses and prostaglandins. The guinea pig bronchi were treated with capsaicin (10 μM) 60 min before the EFS studies. Capsaicin results in a strong tachykinin dependent contraction that returns to baseline in bout

30 min. This capsaicin desenstization treatment prevents subsequent tachykinergic responses to EFS, leaving a neuronal response that is entirely cholinergic in nature (Undem et al., 1990).

The nerves in the tissue were stimulated using electrical field stimulation. Rectangular pulses were delivered to the tissue via the platinum wire electrodes from the Grass S48 stimulator after first being processed by a constant current Med-Lab Stimul-Splitter (Med-Lab Instruments, Fort Collin CO, USA). The square pulses were of 0.1 msec duration with an amplitude of 12V. The impulses were delivered at 8Hz every 1000 seconds. This resulted in rapid and short-lived atropine-sensitive cholinergic contractions. After stable responses were obtained ~5 minutes, the NaV blocker was added until the reduction in response amplitude reached a steady-state at which time a 10-fold larger dose concentrations was added. From data obtained a cumulative concentration response curve was obtained. At the end of the experiment the tissue was maximally contracted with 100 μM carbamylcholine; the EFS contractions were normalized to this maximum response.

The NaV blockers did not inhibit the contractions to the exogenously applied cholinergic agonist carbamylcholine (100 μM); the contractions averaged 3.6 ± 0.7 g, 5.4 ± 3 g and 4.3 ± 0.9 g, and 5.7 ± 1.2 g in vehicle (n=9), TTX (1μM, n= 6), compound 801 (1 μM, n=8), and compound 13 (10 μM, n=7) treated tissues, respectively (P>0.1 ANOVA). In two experiments we evaluated the concentration-response curve of carbamycholine-induced contractions in vehicle, TTX, compound 801, and compound 13 treated tissues and found them to be nearly superimposable (EC5O values averaged 48 nM, 32 nM, 28 nM, and 49 nM, respectively).

*Mouse Trachea*

Mouse tracheal rings, two per animal were prepared exactly as previously described (Weigand LA, 2009). Indomethacin (3 μM) and propranolol (1 μM) was included in the Kreb's bicarbonate buffer. The field stimulation protocol was the same as described above for guinea pig bronchi

except there was a 5 min interval between two consecutive 8 Hz stimulations (in preliminary studies we noted that without such an interval there was a gradual run down of the cholinergic responses over time).

*Human Bronchi*

Lungs were obtained from human organ donors through the International Institute for the Advancement of Medicine program (Exton, PA, USA). The tissue is immediately placed in chilled (Lactated Ringers solution) and shipped overnight arriving in our laboratory 12-24 h later. Once received the lungs were placed in 4 L of chilled oxygenated Kreb's bicarbonate buffer solution (see above). Central bronchi (3mm-5mm inner diameter) are dissected free, trimmed of extraneous tissue and prepared for EFS induced isometric study as described for the guinea pig bronchi and in more detail here (Ellis and Undem, 1992).

*Analysis of NaV1 subunits expression in parasympathetic ganglion neurons*

Parasympathetic ganglia: The animals were killed with $CO_2$ followed by exsanguination, and the trachea, main bronchi and lungs with attached vagus nerves were dissected in $O_2/CO_2$ gassed Krebs solution and pinned dorsal side up under stereomicroscope. Parasympathetic ganglia were identified along vagal branches, dissected and collected with the tip of sharp glass electrode (pulled with Sutter P-2000 puller) and transferred into PCR tube containing RNAse inhibitor (RNaseOUT 1µl, Life Technologies), frozen on dry ice and stored at -80$^{o}$C. A sample of non-ganglion tissue of similar area (~400µm x400µm) and depth of juxtaposed to each ganglion was collected in an identical manner as a negative control. This negative control tissue would be expected to contain mainly adipocytes, some axons, fibroblasts, microvasculature, but no neurons or satellite cells. First strand cDNA was synthesized using the Super-Script III CellsDirect cDNA Synthesis System (Life Technologies) according to the manufacturer's recommendations. Samples were defrosted, lysed (10min, 75°C) and treated with DNAse I, poly(dT) and random hexamer primers (Roche Applied Bioscience) added, reverse transcribed

by SuperscriptIII RT for cDNA synthesis. 2µl of each sample were used for PCR amplification by the HotStar Taq Polymerase Kit (Qiagen) according to the manufacturer's recommendations in a final volume of 20µl. After an initial activation step of 95°C for 15min, cDNAs were amplified with custom-synthesized primers (Life Technologies) by 50 cycles of denaturation at 94°C for 30s, annealing at 60°C for 30s and extension at 72°C for 1 min followed by a final extension at 72°C for 10min. Products were visualized in ethidum-bromide stained 1.5% agarose gels with a 50bp or 100bp DNA ladder. Figures were prepared from multiple original gel images by using Microsoft PowerPoint and Apple Preview. The bands indicate only the presence or absence of a product (i.e. target expression), but not the intensity of expression.

Intron-spanning primers specific for each guinea pig, human, and mouse, $Na_V$ α subunit were designed based on Pubmed sequences with aid of UCSC Genome Browser using Primer3 (v.0.4.0) program (tables 1-3) (Rozen and Skaletsky, 2000). The selectivity of each primer was evaluated by aligning all $Na_V$ subunits with the primer using ClustalW. Positive control RNA was selected based on established $Na_V$ subunit expression pattern: whole brain RNA for $Na_V$ 1.1, 1.2, 1.3 and 1.6, skeletal muscle RNA for $Na_V$ 1.4, heart muscle RNA for $Na_V$ 1.5 and DRG or vagal sensory ganglia RNA for $Na_V$ 1.7, 1.8 and 1.9. The guinea pig and mouse RNA was isolated by using RNAeasy mini kit (Qiagen). Human RNA was purchased from Clontech.

*Electrophysiology*

Human Nav1,1, hNav1.2, hNav1.3, hNav1.6, and hNav1.7 stably expressedin HEK cells were obtained from Millipore, and cultured according to manufactures specifications. Mouse Nav1.7, rat Nav1.7 and gpNav1.7-HEK cell lineswere generated at Lilly Laboratories. The media consisted of: DMEM (High Glucose), FBS (10%) (Heat inactivated), HEPES (20 mM) Glutamax 2 mM, Pen/Strep 1%, G418 (0.3mg/ml) (all obtained from Gibco).

JPET Fast Forward. Published on January 30, 2017 as DOI: 10.1124/jpet.116.238469
This article has not been copyedited and formatted. The final version may differ from this version.



a.Whole-cell voltage clamp experiments were performed at room temperature, using a Multiclamp 700B amplifier, Digidata 1440A interface and pClamp 10.0 software to obtain IC50 for the NaV blockers. For experiments using hNav1.7, mNav1.7 the external solution contained (mM): NaCl 40, Choline-Cl 100, KCl 5.4, $CaCl_2$ 1.8, $MgCl_2$ 0.8, HEPES 10, Glucose 5, pH 7.4 adjusted with N-methyl d-glutamine (NMDG), (osmolarity, 300 mOsm). For experiments using hNav1.6 and mNav1.6 the external solution contained (mM): NaCl 138, KCl 5.4, $CaCl_2$ 1.8, $MgCl_2$ 0.8, HEPES 10, Glucose 5, pH 7.4 adjusted with NaOH, (osmolarity, 300 mOsm). Micropipettes were pulled from borosilicate glasses with a Sutter P-97 puller. Pipette solutions contained (mM): CsF 110, CsCl 20, NaCl 10, EGTA 1.1, HEPES 10, pH 7.2 adjusted with CsOH, (osmolarity, 294 mOsm). Electrodes had a resistance of 1.5-2 MΩ when filled with pipette solution. After seal rupture, series resistance (<5 MΩ**)** was compensated (70–80%) and periodically monitored. Test compounds are diluted in DMSO at final stock concentration of 10mM. Working dilutions were also done using DMSO and the final concentration was tested at a 0.1% DMSO concentration. A steady-state inactivation (SSI) curve is run at a holding potential of -130mV using a 10 second pre-pulse ranging from -130mV to -30mV in 10mV steps followed by a test pulse to -10mV for 10ms at 0.06Hz intervals. The data is then fit to a Boltzman Sigmoidal to calculate the $V_{0.5}$ using Prism and the following formula:

$$Y=Bottom+(Top-Bottom)/(1+exp((V_{0.5}-X)/Slope))$$

where Y= Current measured at the test pulse, X= Pre-pulse potential.

The SSI curve was repeated every 2 minutes until peak current baselines are stable. The holding potential is then changed to a potential near the calculated $V_{0.5}$ and held for 1 minute. The protocol is then run from the new holding potential then stepped to -10mV for 10ms at 0.1Hz intervals. After a stable baseline is achieved, the test compound is superfused onto the cell until a new equilibrium is established. Percent Inhibition is determined as ((Control-

JPET Fast Forward. Published on January 30, 2017 as DOI: 10.1124/jpet.116.238469
This article has not been copyedited and formatted. The final version may differ from this version.



Drug)/Control)*100. Compound potencies are calculated with a logistic fit using Prism 6.03 (GraphPad) with Equation 2: Y=Bottom + (Top-Bottom)/(1+10^((LogEC50-X)*HillSlope)) Where X is the logarithm of the test concentration and Y is the Percent Inhibition.

b. Compound 13 selectivity was assessed at Essen Bioscience using human Nav1.1, Nav1.2, hNav1.4, hNav1.5, hNav1.6, and hNav1.7 transfected in HEK cells and Ion Works Barracuda as electrophysiology platform using PPC (Population Patch Clamp) mode. Compound potency was assessed by using functional selectivity protocols consisting in the application of different trains of depolarizations that cycle channels through states that are most representative of pathology for hNav 1.7 and physiology for the rest.Voltage protocols follow the same time scheduled, being applied once in the absence of compound, then in the presence of compound, 5 minutes after addition, and then five more times every one minute.

The external recording solution comprised (in mM): 137 NaCl, 4 KCl, 10 HEPES, 1 MgCl2, 1.8 CaCl2 and pH7.3 with NaOH. The internal solution comprised (in mM): 90 K-gluconate, 40 CsCl, 10 NaCl, 3.2 EGTA, 5 HEPES, 3.2 MgCl2 and pH 7.3 with KOH. All buffer constituents were obtained from Sigma-Aldrich. Electrical access was achieved using amphotericin (120 μg $ml^{-1}$) in the internal solution to obtain the perforated-patch clamp configuration.

Compounds were solubilized in DMSO containing 6% pluronic F127 (Sigma) as 10 mM stock solutions. A 11 point 1:3 cross-plate dilution was carried out in DMSO (6% pluronic), diluted 1/300 in external solution and the added to assay plate using dual addition mode from mid position without mixing to reduce nonspecific binding and improve compound exposure.

Peak inward currents were determined from the first and last depolarizing pulses. % Inhibition values were calculated according to the following equation, using peak currents obtained in the absence (pre) and presence (post) of test compound (last train): Concentration response curves were fitted to a four parameter logistic fit. Data was analysed using IonWorks Barracuda software (v2.5.0.280), Microsoft Excel (v7.0), XLFit (IDBS, v5.2.0.0) and GraphPad prism (v5).

JPET Fast Forward. Published on January 30, 2017 as DOI: 10.1124/jpet.116.238469
This article has not been copyedited and formatted. The final version may differ from this version.



Drugs and solutions

Drugs were prepared fresh as 0.1mM stock solutions. Compound 801 was identified in Icagen/Pfizer patent WO2010079443 and synthesized at Lilly Laboratories (Indianapolis, in USA) and dissolved in DMSO

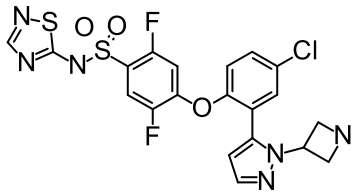

Compound 13 was first described in WO2012004706. It was synthesized at Almirall Laboratories (Barcelona, SPAIN) and dissolved in DMSO.

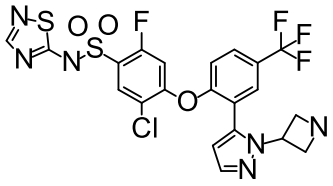

ICA121431 (Tocris Labs) and PF-01247324 (Sigma) was dissolved in DMSO. Tetrodotoxin (Alamone Labs) and propranolol (Sigma) were dissolved in water; indomethacin (Sigma) was prepared in ethanol.

**Results**

In the patch-clamp analysis of various NaV1 currents, TTX inhibits NaV 1.1, 1.2, 1.3, 1.6, and 1.7 with similar potency with IC50 values in the 1-10 nM range. ICA-121431, by contrast potently blocks NaV 1.1, 1.2 and 1.3, but has little effect on 1.6 or 1.7. We noted, for example, that the guinea pig NaV1.7 current was inhibited less than 20% even at 10 μM ICA-121431. Compound 801 and Compound 13 are arylsulfonamides closely related to other selective NaV1.7 blockers (Alexandrou et al., 2016). We found Compound 801 to be a potent NaV1.7 blocker, being 5-10 fold more potent at this channel than NaV 1.2 and NaV 1.6. Compound 801 was equally potent against human and guinea pig NaV1.7. Compound 13 was selective for blocking NaV1.7 with little affinity for NaV 1.2, 1.3, or 1.6, and was found to be more potent at human vs guinea pig NaV1.7 (these data are summarized in table 4).



Guinea Pig Bronchi

TTX, Compound 801, and Compound 13 each effectively blocked the neuronally evoked cholinergic contractions of the guinea pig bronchi with IC50s of 8.4, 56, and 480 nM, respectively. In contrast, ICA121431 at concentrations that would be expected to fully block NaV1.1, 1.2 and 1.3 was virtually devoid of an inhibitory effect on the cholinergic contractions. These data are illustrated in Fig. 1. As expected, PF-01247324, a drug that selectively blocks the TTX-resistant NaV 1.8 channels, had no effect on the cholinergic contractions (34 ±3% vs 35±3% in the absence and presence of 1 μM of the drug, respectively; n=6, P>0.1) (Payne et al., 2015).

NaV1 gene expression was detected in bronchial ganglia (n=11), but not in the juxtaposed non-neuronal tissue. NaV1.7 was the only TTX-sensitive channel mRNA expressed in most guinea

pig airway-associated parasympathetic ganglia. NaV1.7 was expressed in 10/11 isolated ganglia. The only other TTX-sensitive channel expressed was NaV 1.3, and this was expressed in only 2/11 ganglia. Interestingly, NaV1.9 was also expressed in 8/11 ganglia. These data are shown in Fig 1. Inasmuch as NaV1.9 is a TTX-resistant channel, these data support the hypothesis based on our functional studies that NaV1.7 provides the functional control over action potential discharge in postganglionic parasympathetic nerves in the guinea pig airways.

Mouse Trachea

TTX potently (IC50 21nM) blocked neuronally evoked cholinergic contractions of the mouse trachea. In contrast to guinea pig airways, none of the selective NaV1 blockers when studied alone inhibited the cholinergic responses. However, in the presence of NaV1.1, 1.2, 1.3 blockade with ICA-121431 (10 μM), either Compound 13 or Compound 801 was able to abolish the contractions in a concentration-dependent fashion. Thus, to block parasympathetic responses in the mouse airway both NaV1.7 and NaV1.1, 1.2 and/or NaV1.3 had to also be blocked. These data are illustrated in Fig. 2.

We evaluated NaV1 gene expression in 5 ganglia isolated from mouse airways. Consistent with the functional studies, The NaV1 expression was more extensive then in guinea pig ganglia. With respect to TTX-sensitive channels NaV1.1, NaV1.3, NaV1.6, and NaV1.7 was expressed by neurons in 100%, 80%, 40% and 60% of the ganglia, respectively. With respect to TTX-resistant channels, NaV1.9 was expressed in 3/5 ganglia (Fig.2).

Human Bronchi

The large differences in the NaV1 regulating airways parasympathetic responses between guinea pig and mice begs the question as to which laboratory animal is the more translatable to the human condition. Like the guinea pig and mouse, the neuronally-evoked cholinergic

contractions were potently and effectively blocked by TTX. Blocking NaV1.1, 1.2 and 1.3 with ICA-121431 had no effect on the cholinergic responses whereas either Compound 801 or Compound 13 mimicked the TTX response (Fig. 3). Consistent with our potency predictions obtained with patch clamp electrophysiological studies of human vs guinea pig NaV1.7 in heterologous systems (table 1), Compound 13 was more potent in blocking the parasympathetic contractions in human bronchi than guinea pig bronchi (Fig 1 and Fig. 3).

We evaluated the NaV1 gene expression in 5 ganglia isolated from the bronchi of 3 human donors. NaV 1.7 mRNA was expressed in every parasympathetic ganglia, whereas other TTX-sensitive NaV1s were largely unexpressed with the exception of NaV 1.3 which was found in only 1 of 5 ganglia (Fig. 3).

## Discussion

The functional and mRNA expression data support the hypothesis that neurotransmission in parasympathetic postganglionic neurons innervating smooth muscle in human and guinea pig airways is under the control of NaV1.7. On the other hand in the mouse, the most commonly employed laboratory animal for investigations into both NaV1 biology and respiratory physiology, the parasympathetic neurons were under redundant control of NaV1.7 and 1.1 and/or 1.3. One must therefore be cautious when drawing NaV1 related conclusions about human autonomic nerves from physiological studies carried out exclusively in mice.

NaV1.9 was expressed along with NaV 1.7, especially in guinea pig parasympathetic neurons. That TTX and the selective NaV1.7 blockers could abolish the parasympathetic response indicated that NaV 1.9 is not sufficient for driving action potential discharge and acetylcholine release from the terminals. This is as would be expected based on its biophysical properties, but it may play a role in regulating the electrical excitability of the neurons.

The potency of NaV blockers in blockers in isolated tissues is generally less than that seen in patch-clamp electrophysiological studies. There are several potential reasons for this. First, the concentration of the inhibitor in the tissue bath solution may not reflect that concentration in the biophase of the nerve endings. To minimize this issue we incubated the blocking drug for a period sufficient such that the inhibitory effect reached a steady-state. Secondly, the potency of NaV blockers including aryl sulfonamide blockers such as compounds 801 and 13, can be dramatically influenced by the biophysical state of the channel (Alexandrou et al., 2016). The state of the channel (e.g. relative extent of inactivation) can be specifically manipulated in patch-

clamp conditions, but remains unknown in channels inserted within nerve membranes in tissues. Finally, the beta subunit composition may potentially influence the pharmacology of the NaV blockers (Wilson et al., 2015), and this may differ in channels expressed in heterologous system vs channels in the parasympathetic nerves within tissues. In the present study it is noteworthy that the potency of the selective NaV1.7 blockers *relative* to TTX was similar in the tissue assay and patch-clamp analysis.

Alterations in both the sensory and parasympathetic nervous systems likely contribute to airway pathologies such as asthma and COPD (reviewed in (Undem and Potenzieri, 2012; Mazzone and Undem, 2016)). That NaV1.7 is the dominant controller of neurotransmission in human and guinea pig airway parasympathetic neurons provides for a strategy of limiting parasympathetic tone in the respiratory tract via selective NaV1.7 blockade. Topically administered anti-muscarinic drugs are presently used to decrease cholinergic tone in the airways of those suffering from asthma or COPD. Blocking NaV 1.7 is an orthogonal approach to diminish cholinergic contractions and may have the added benefit of not only blocking the release of acetylcholine but also other parasympathetic transmitters including for example VIP and nitric oxide that provide pro-mucus secretory activities (Baker et al., 1985; Wine, 2007). The VIP/nitric oxide containing postganglionic nerves in the guinea pig airways, however, are derived from parasympathetic neurons distinct from the cholinergic neurons(Canning and Undem, 1993), and therefore may reveal distinct NaV1 channel expression. The airway parasympathetic ganglia are mainly associated with larger central airways. The neurons within these ganglia then project postganglionic nerves to the smooth muscle of bronchi and bronchioles (Undem and Potenzieri, 2012). Another speculative benefit therefore of topically applied (inhaled) NaV blocking drugs over muscarinic receptor antagonists is that even central deposition of an NaV blocker my lead to bronchodilation of more peripheral bronchi and bronchioles. Finally, we have recently reported that blocking NaV1.7 can inhibit action potential conduction along sensory C-fibers in

the respiratory tract leading to inhibition of undesirable sensations such as dyspnea and urge to cough; an effect that anti-muscarinic drugs would not share (Muroi et al., 2011; Muroi et al., 2013). It should be kept in mind that the present study focused on airways from healthy laboratory animals and donors that did not have asthma or COPD; both the expression and function of NaV channels may potentially be altered in the diseased state (Chahine and O'Leary, 2014).

There has been intensive efforts in developing selective NaV1.7 blockers for the treatment of pain (Dib-Hajj et al., 2013). As far as we know this is the first study on the NaV1 expression and function in parasympathetic neurons. If our observations in the respiratory tract hold true for other visceral organs it may suggest new indications for NaV1.7 blockers. The findings may also explain potential anti-parasympathetic side-effects for systemically acting NaV1.7 blockers.

Individuals with loss of function and gain of mutations in NaV1.7 have been identified (Dib-Hajj et al., 2005; Goldberg et al., 2007). These people suffer from a congenital insensitivity to pain or erythomelalgia, respectively. Loss of function mutation also lead to a decreased sensitivity of smell (Weiss et al., 2011). Based on the present data, one might predict that those with loss of function mutations may experience less reflex bronchial contractions and secretions, and perhaps less airway reactive disease like asthma, but this hypothesis has yet to be addressed.



*Author Contributions*

*Participation in research design*: Kocmalova, Kollarik, Canning, Undem

*Conducted experiments*: Kocmalova, Kollarik, Ru, Herbstromer, Meeker, Fonqluerna, Aparici, Miralpeix, Ch, Li, Wilenkin, McDermott, Krajewski

*Contributed new reagents*: Krajewski, Fonquerna, Miralpeix

*Performed data analysis*: Kocmalova, Kollarik, Undem, Krjewski, Aparici, Miralpeix

*Wrote or contributed to writing the manuscript*: Kocmalova, Kollarik, Krajweski, Undem

**References**

Alexandrou AJ, Brown AR, Chapman ML, Estacion M, Turner J, Mis MA, Wilbrey A, Payne EC, Gutteridge A, Cox PJ, Doyle R, Printzenhoff D, Lin Z, Marron BE, West C, Swain NA, Storer RI, Stupple PA, Castle NA, Hounshell JA, Rivara M, Randall A, Dib-Hajj SD, Krafte D, Waxman SG, Patel MK, Butt RP and Stevens EB (2016) Subtype-Selective Small Molecule Inhibitors Reveal a Fundamental Role for Nav1.7 in Nociceptor Electrogenesis, Axonal Conduction and Presynaptic Release. *PLoS One* **11**:e0152405.

Baker B, Peatfield AC and Richardson PS (1985) Nervous control of mucin secretion into human bronchi. *J Physiol* **365**:297-305.

Canning BJ and Undem BJ (1993) Evidence that distinct neural pathways mediate parasympathetic contractions and relaxations of guinea-pig trachealis. *J Physiol* **471**:25-40.

Catterall WA, Goldin AL and Waxman SG (2005) International Union of Pharmacology. XLVII. Nomenclature and structure-function relationships of voltage-gated sodium channels. *Pharmacol Rev* **57**:397-409.

Chahine M and O'Leary ME (2014) Regulation/modulation of sensory neuron sodium channels. *Handb Exp Pharmacol* **221**:111-135.

Dib-Hajj SD, Rush AM, Cummins TR, Hisama FM, Novella S, Tyrrell L, Marshall L and Waxman SG (2005) Gain-of-function mutation in Nav1.7 in familial erythromelalgia induces bursting of sensory neurons. *Brain* **128**:1847-1854.

Dib-Hajj SD, Yang Y, Black JA and Waxman SG (2013) The Na(V)1.7 sodium channel: from molecule to man. *Nat Rev Neurosci* **14**:49-62.

Ellis JL and Undem BJ (1992) Antigen-induced enhancement of noncholinergic contractile responses to vagus nerve and electrical field stimulation in guinea pig isolated trachea. *J Pharmacol Exp Ther* **262**:646-653.

Goldberg YP, MacFarlane J, MacDonald ML, Thompson J, Dube MP, Mattice M, Fraser R, Young C, Hossain S, Pape T, Payne B, Radomski C, Donaldson G, Ives E, Cox J, Younghusband HB, Green R, Duff A, Boltshauser E, Grinspan GA, Dimon JH, Sibley BG, Andria G, Toscano E, Kerdraon J, Bowsher D, Pimstone SN, Samuels ME, Sherrington R and Hayden MR (2007) Loss-of-function mutations in the Nav1.7 gene underlie congenital indifference to pain in multiple human populations. *Clin Genet* **71**:311-319.

Mazzone SB and Undem BJ (2016) Vagal Afferent Innervation of the Airways in Health and Disease. *Physiol Rev* **96**:975-1024.

McCormack K, Santos S, Chapman ML, Krafte DS, Marron BE, West CW, Krambis MJ, Antonio BM, Zellmer SG, Printzenhoff D, Padilla KM, Lin Z, Wagoner PK, Swain NA, Stupple PA, de Groot M, Butt RP and Castle NA (2013) Voltage sensor interaction site for selective small molecule inhibitors of voltage-gated sodium channels. *Proc Natl Acad Sci U S A* **110**:E2724-2732.

Muroi Y, Ru F, Chou YL, Carr MJ, Undem BJ and Canning BJ (2013) Selective inhibition of vagal afferent nerve pathways regulating cough using Nav 1.7 shRNA silencing in guinea pig nodose ganglia. *Am J Physiol Regul Integr Comp Physiol* **304**:R1017-1023.

Muroi Y, Ru F, Kollarik M, Canning BJ, Hughes SA, Walsh S, Sigg M, Carr MJ and Undem BJ (2011) Selective silencing of Na(V)1.7 decreases excitability and conduction in vagal sensory neurons. *J Physiol* **589**:5663-5676.

Payne CE, Brown AR, Theile JW, Loucif AJ, Alexandrou AJ, Fuller MD, Mahoney JH, Antonio BM, Gerlach AC, Printzenhoff DM, Prime RL, Stockbridge G, Kirkup AJ, Bannon AW, England S, Chapman ML, Bagal S, Roeloffs R, Anand U, Anand P, Bungay PJ, Kemp M, Butt RP and Stevens EB (2015) A novel selective and orally bioavailable Nav 1.8 channel blocker, PF-01247324, attenuates nociception and sensory neuron excitability. *Br J Pharmacol* **172**:2654-2670.

Priest BT and Kaczorowski GJ (2007) Subtype-selective sodium channel blockers promise a new era of pain research. *Proc Natl Acad Sci U S A* **104**:8205-8206.

Rozen S and Skaletsky J (2000) Primer3 on the WWW for general users and for biologist programmers, in *Bioinformatics Methods and Protocols: Methods in Molecular Biology* (Krawetz S and Misener S eds) pp 365-386, Humana Press, Totowa.

Undem BJ, Myers AC, Barthlow H and Weinreich D (1990) Vagal innervation of guinea pig bronchial smooth muscle. *J Appl Physiol (1985)* **69**:1336-1346.

Undem BJ and Potenzieri C (2012) Autonomic neural control of intrathoracic airways. *Compr Physiol* **2**:1241-1267.

Waxman SG (2013) Painful Na-channelopathies: an expanding universe. *Trends Mol Med* **19**:406-409.

Weigand LA MA, Meeker S, Undem BJ (2009) Mast cell-cholinergic nerve interaction in mouse airways. *J Physiol* **587**:3355-3362.

Weiss J, Pyrski M, Jacobi E, Bufe B, Willnecker V, Schick B, Zizzari P, Gossage SJ, Greer CA, Leinders-Zufall T, Woods CG, Wood JN and Zufall F (2011) Loss-of-function mutations in sodium channel Nav1.7 cause anosmia. *Nature* **472**:186-190.

Wilson MJ, Zhang MM, Gajewiak J, Azam L, Rivier JE, Olivera BM and Yoshikami D (2015) Alpha- and beta-subunit composition of voltage-gated sodium channels investigated with mu-conotoxins and the recently discovered muO section sign-conotoxin GVIIJ. *J Neurophysiol* **113**:2289-2301.

Wine J (2007) Parasympathetic control of airway submucosal glands: central reflexes and the airway intrinsic nervous system. *Auton Neurosci* **133**:35-54.

JPET Fast Forward. Published on January 30, 2017 as DOI: 10.1124/jpet.116.238469
This article has not been copyedited and formatted. The final version may differ from this version.



Footnote

This work was supported by the Heart and Blood Institute of the National Institutes of Health Grant [R01HL122228] and by Biomedical Center Martin Grant [ITMS 26220220187], Slovakia.

Figure Legends

**Figure 1.** (a-e) Effect of $Na_V$ inhibitors on airway efferent parasympathetic nerves in the guinea pig. (a) Representative trace of the effect of TTX on bronchial contractions evoked by activation of parasympathetic nerves with electrical field stimulation (EFS, 16Hz for 10s, repeated every 60s, denoted by bullets). Effect of (b) TTX, (c) Compound 801, (d) Compound 13 and (e) ICA121431 on EFS-induced bronchial contractions, n=6. (f-g) Collection of parasympathetic neurons for RT-PCR. (f) Parasympathetic ganglion in the guinea pig airway. The highlighted area is magnified in (g). Some of the parasympathetic neurons are denoted by asterisks. The ganglion was dissected and collected into PCR tube. A sample from the neighboring tissue was collected as a negative control. (h-i) Expression of $Na_V$ 1.1-1.9 subunits in parasympathetic neurons in the guinea pig. (h) Representative PCR gel. G1-G6, individual parasympathetic ganglia, N1-N6, corresponding negative controls. The arrows indicate expected product size. Note: $Na_V$1.4 in G6 sample is counted as negative because of incorrect size. (i) Percentage of NaV subunit expression in parasympathetic ganglia (n=11).

**Figure 2.** (a-f) Effect of $Na_V$ inhibitors on airway efferent parasympathetic nerves in the mouse. The effect of (a) TTX, (b) Compound 801, (c) Compound 13, (d) ICA121431, and ICA121431 (10μM) in combination with (e) Compound 801 (f) and Compound 13 (f) on the he EFS-induced bronchial contractions, n=6. (g) Expression of $Na_V$ 1.1-1.9 subunits in parasympathetic neurons in the mouse. G1-G5, individual ganglia, +, positive control, -, negative control. The arrows indicate expected product size.

**Figure 3.** (a-e) Effect of $Na_V$ inhibitors on airway efferent parasympathetic nerves in the human. (a) Representative trace of the effect of TTX on bronchial contractions evoked by activation of parasympathetic nerves with electrical filed stimulation (EFS, 16Hz for 10s, repeated every 60s, denoted by bullets). Effect of (b) TTX, (c) Compound 801, (d) Compound 13 and (e) ICA121431 on EFS-induced bronchial contractions, n=6. (f) An example of human parasympathetic ganglion (arrow). (g) Magnified area from the ganglion shown in (f). Some of the parasympathetic neurons are denoted by asterisks. (h) Expression of $Na_V$ 1.1-1.9 subunits in human isolated parasympathetic ganglia. G1-G6, individual ganglia, +, positive control. The arrows indicate expected product size.

JPET Fast Forward. Published on January 30, 2017 as DOI: 10.1124/jpet.116.238469
This article has not been copyedited and formatted. The final version may differ from this version.



Table 1. **The guinea pig primer sequences for single cell RT-PCR**

| Target | Primer | Sequence (5' to 3') | Product size (bp) | Genomic size (bp) | NCBI Reference Sequence: |
|---|---|---|---|---|---|
| ß-actin | Forward | TCTCTTCCAGCCCTCCTTC | 373 | N/A | NT_176389.1 |
| | Reverse | GTCCTCAAAGGTGCTGTGCT | | | |
| $Na_V1.1$ | Forward | AAGGGTTTCGCTTCTCCATT | 206 | >1000 | XM_003478553.2 |
| | Reverse | GTCCTCAAAGGTGCTGTGCT | | | |
| $Na_V1.2$ | Forward | GAGACTTCAGTGGTGCTGGTG | 265 | N/A | XM_003478556.2 |
| | Reverse | AGCAGAGACTGGTGTGGAGAA | | | |
| $Na_V1.3$ | Forward | ACACAACAGAGGAGAGGCAGA | 171 | >1000 | XM_003478666.2 |
| | Reverse | CGTCTTGGGGAGAATAGGG | | | |
| $Na_V1.4$ | Forward | GGCTCTCCCTCCACCATC | 159 | N/A | XM_003465929.1 |
| | Reverse | CAGCGGTTTCTTGCCATC | | | |
| $Na_V1.5$ | Forward | GTCATTTTCCTGGGCTCCTT | 245 | >1000 | XM_005001107.1 |
| | Reverse | TTGCTCCTTCTCTCGTGGTT | | | |
| $Na_V1.6$ | Forward | CCTCCTATGGACGAAAAGACA | 222 | >1000 | XM_005006531.1 |
| | Reverse | TGCAGATGGTGATAGCCAAG | | | |
| $Na_V1.7$ | Forward | GAGGAAAAGGGAGATGATGAGA | 158 | >1000 | XM_003478661.2 |
| | Reverse | AACAGGGAGCCACGAATG | | | |
| $Na_V1.8$ | Forward | CGGAAAGGTGACAATGGAG | 187 | >1000 | XM_003464141.2 |
| | Reverse | AGCAGGGACAGTAGCGAAGA | | | |
| $Na_V1.9$ | Forward | GTTCCAGGTTCCCAAATCAA | 162 | >1000 | XM_003464142.2 |
| | Reverse | GAGGCAGAAGAGGGTGAGG | | | |

*N/A indicates no match in UCSC In-Silico PCR

JPET Fast Forward. Published on January 30, 2017 as DOI: 10.1124/jpet.116.238469
This article has not been copyedited and formatted. The final version may differ from this version.



Table 2. **The human primer sequences for single cell RT-PCR**

| Target | Primer | Sequence (5' to 3') | Product size (bp) | Genomic size (bp) | NCBI Reference Sequence: |
|---|---|---|---|---|---|
| ß-actin | Forward | AGAAAATCTGGCACCACACC | 188 | 629 | NM_001101.3 |
| | Reverse | AGAGGCGTACAGGGATAGCA | | | |
| $Na_V1.1$ | Forward | TCAGTTCCTACATCGCCTGTT | 174 | >1000 | NM_001165963.1 |
| | Reverse | ACTCATTGCTCGTTGCCTTT | | | |
| $Na_V1.2$ | Forward | GTGCTGGTGGGATAGGAGTT | 288 | N/A | NM_021007.2 |
| | Reverse | TGCGTCTTGGAGAGAAAAGG | | | |
| $Na_V1.3$ | Forward | GGAACCGAAGGAAGAAAAGAA | 252 | N/A | NM_006922.3 |
| | Reverse | CCCGACCTCTGAAACTGAAA | | | |
| $Na_V1.4$ | Forward | TCAACAACCCCTACCTGACC | 208 | >1000 | NM_000334.4 |
| | Reverse | TTCTCCTCTGCCTGCTCCT | | | |
| $Na_V1.5$ | Forward | CTAAAGGCAGGCGAGAACC | 188 | 708 | NM_198056.2 |
| | Reverse | AGGTAGAAGGACCCCAGGAA | | | |
| $Na_V1.6$ | Forward | CGTCTTGGTCATCTTTGTGG | 242 | >1000 | NM_014191.3 |
| | Reverse | CCCCTCCTTCTTCACCTTCT | | | |
| $Na_V1.7$ | Forward | TGGAGAGGAAAAGGGAGATG | 166 | >1000 | NM_002977.3 |
| | Reverse | AGAAAACAAGGAGCCACGAA | | | |
| $Na_V1.8$ | Forward | TAAGCGAGGCACTTCTGACC | 144 | >1000 | NM_006514.3 |
| | Reverse | GAGAGGAAAGCCCAAGCAA | | | |
| $Na_V1.9$ | Forward | GGCAAGAGGTTTCATTCTGG | 125 | >1000 | NM_014139.2 |
| | Reverse | GGGGCAATAGTTTGATGGTG | | | |

*N/A indicates no match in UCSC In-Silico PCR

JPET Fast Forward. Published on January 30, 2017 as DOI: 10.1124/jpet.116.238469
This article has not been copyedited and formatted. The final version may differ from this version.



Table 3. **The mouse primer sequences for single cell RT-PCR**

| Target | Primer | Sequence (5' to 3') | Product size (bp) | Genomic size (bp) | NCBI Reference Sequence: |
|---|---|---|---|---|---|
| ß-actin | Forward | GTGGGAATGGGTCAGAAGG | 302 | 756 | NM_007393.3 |
| | Reverse | GAGGCATACAGGGACAGCA | | | |
| $Na_V1.1$ | Forward | AGACAGCATCAGGAGGAAGG | 118 | >1000 | NM_018733.2 |
| | Reverse | GGAGAACAGGGAACCACGA | | | |
| $Na_V1.2$ | Forward | TTTTCGGCTCATTCTTCACA | 305 | >1000 | NM_001099298.2 |
| | Reverse | CATCTCTTGGCTCTGGTCGT | | | |
| $Na_V1.3$ | Forward | AGACAGAGGGAGCACTTGGA | 200 | >1000 | NM_018732.3 |
| | Reverse | CTATTGCGTCTTGGGGAAAA | | | |
| $Na_V1.4$ | Forward | TCATCTTCCTGGGTTCCTTC | 206 | 941 | NM_133199.2 |
| | Reverse | ATCTGCCTCCTCTCCACCTT | | | |
| $Na_V1.5$ | Forward | TGGGCTCCTTCTACCTTGTG | 247 | >1000 | NM_021544.4 |
| | Reverse | CGTTTCCTCCTCTTGCTCCT | | | |
| $Na_V1.6$ | Forward | AGGCAGCAAAGACAAACTGG | 157 | N/A | NM_001077499.2 |
| | Reverse | GCAGCACTTGAACCTCTGG | | | |
| $Na_V1.7$ | Forward | ATGCTCTTCTTTGCGGTTTC | 381 | >1000 | NM_001290674.1 |
| | Reverse | CGGCTTCTTCCTGCTCTTTT | | | |
| $Na_V1.8$ | Forward | CAATCCGACCCTTACAACCA | 147 | >1000 | NM_001205321.1 |
| | Reverse | AAAGACCCCGTCATCCAAG | | | |
| $Na_V1.9$ | Forward | CAGCTTTGGCTGGTCTTTTC | 228 | >1000 | NM_011887.3 |
| | Reverse | TTCTCCTTGGCCTCTGTCTC | | | |

*N/A indicates no match in UCSC In-Silico PCR

JPET Fast Forward. Published on January 30, 2017 as DOI: 10.1124/jpet.116.238469
This article has not been copyedited and formatted. The final version may differ from this version.



Table 4 Estimated IC50 values (nM) for NaV1 blockers at human NaV1 channels

| | TTX [a] | Cmpd 801 [b] | Cmpd 13 [c] | ICA121431 [d] |
|---|---|---|---|---|
| NaV 1.1 | 6 | 8 | nd | 23 |
| NaV 1.2 | 12 | 6 | 900 | 240 |
| NaV 1.3 | 4 | 460 | >30,000 | 13 |
| NaV 1.6 | 1.6 | 8 | 6900 | 13,000 |
| NaV 1.7 | 6 | 1 | 2 | 12,000 |
| NaV 1.7 (GP) | 2.7 | 4.4 | 16.9 | >10,000 |

[a] All values are for human NaV1 channels except for the guinea pig (GP) NaV 1.7 values. The values for TTX were obtained from (Catterall et al., 2005) except for the the NaV 1.7s which were obtained here as described in methods.

[b] The values for compound 801 were obtained as described in methods

[c] The values for compound 13 were obtained by Ion Works and kindly provided by Dr. Silvia Fonquerna at Almirall laboratories

[d] The values for ICA121431 was obtained from (McCormack et al., 2013)

JPET Fast Forward. Published on January 30, 2017 as DOI: 10.1124/jpet.116.238469
This article has not been copyedited and formatted. The final version may differ from this version.



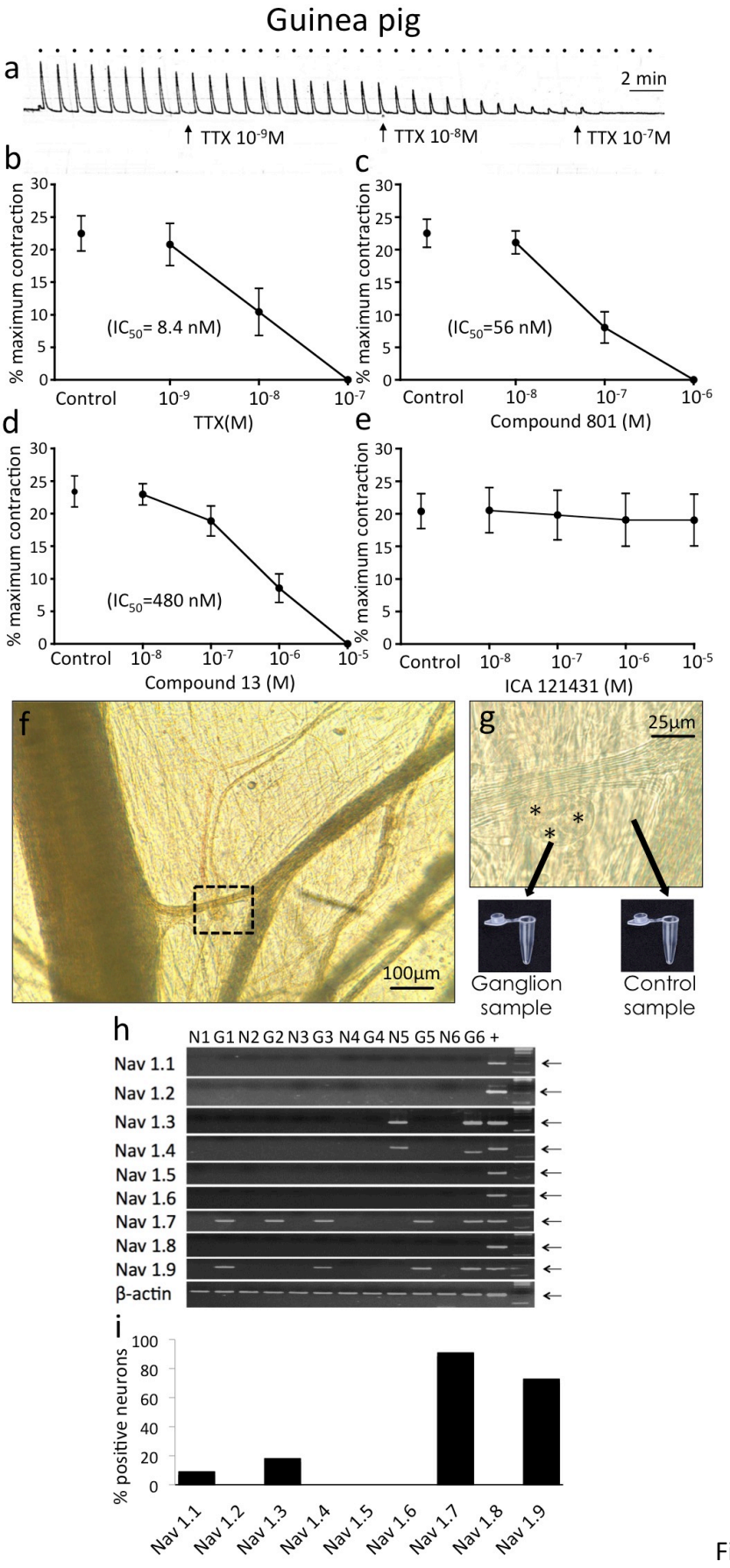


Figure 1

JPET Fast Forward. Published on January 30, 2017 as DOI: 10.1124/jpet.116.238469
This article has not been copyedited and formatted. The final version may differ from this version.



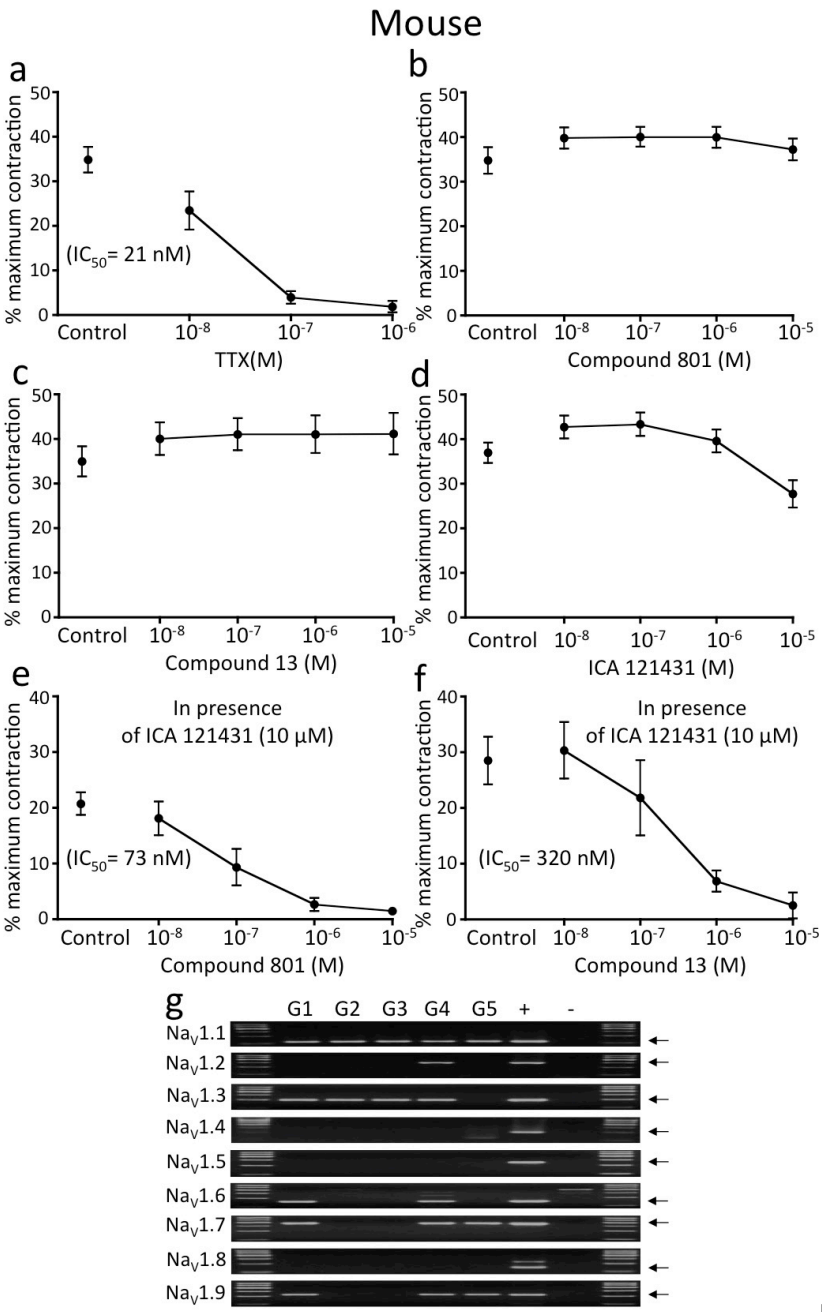


Figure 2

JPET Fast Forward. Published on January 30, 2017 as DOI: 10.1124/jpet.116.238469
This article has not been copyedited and formatted. The final version may differ from this version.



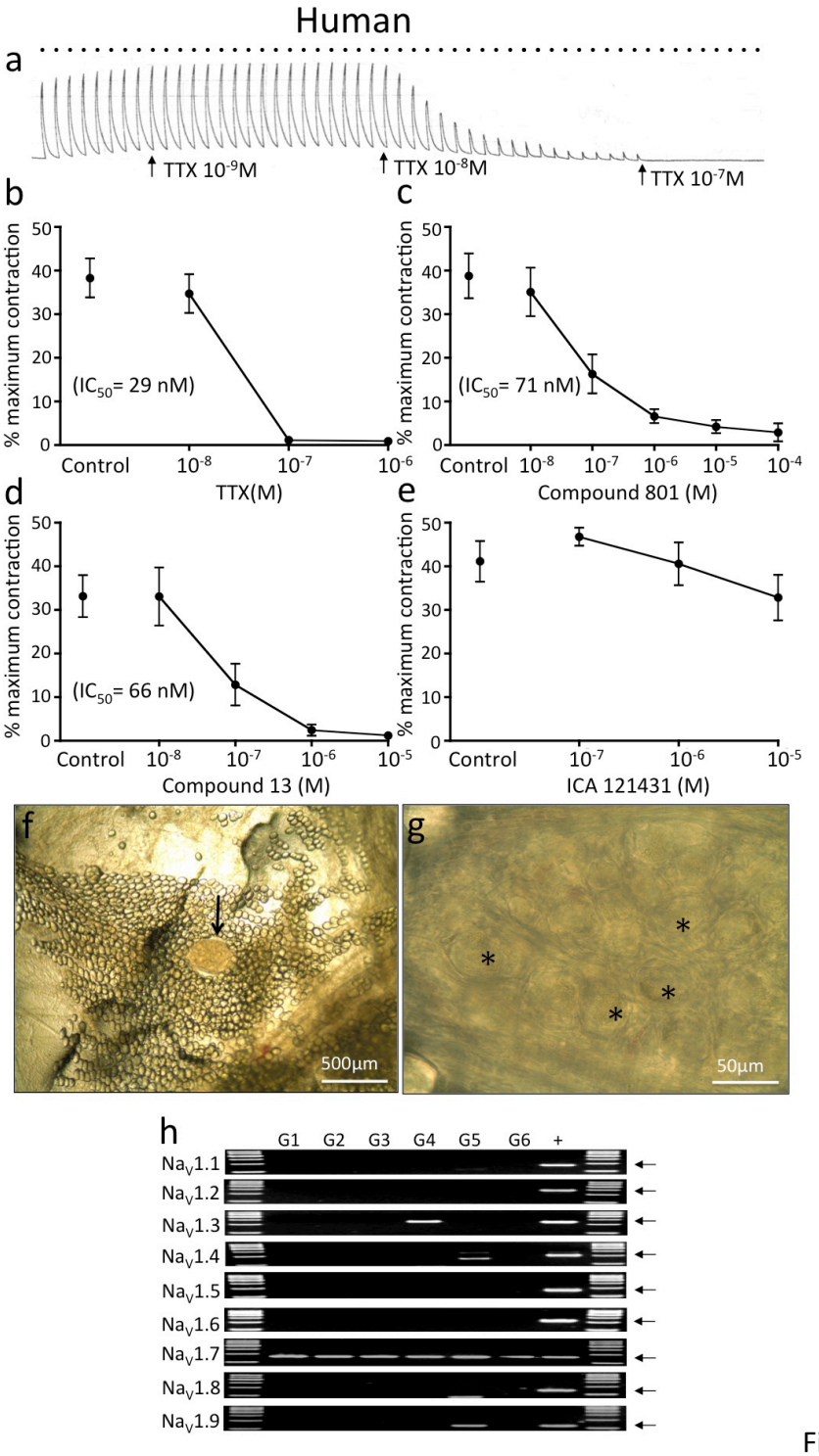


Figure 3